EUROPEAN ORGANIZATION FOR NUCLEAR RESEARCH

CERN EP/2000-086
June 30th, 2000

Search for charged Higgs bosons in e^+e^- collisions at energies up to $\sqrt{s} = 189$ GeV

The ALEPH Collaboration*)

Abstract

The data collected at centre-of-mass energies of 188.6 GeV by ALEPH at LEP, corresponding to an integrated luminosity of 176.2 pb^{-1}, are analysed in a search for pair-produced charged Higgs bosons $H^{\pm}$. Three analyses are employed to select the $\tau^+\nu_\tau\tau^-\bar{\nu}_\tau$, $c\bar{s}\tau^-\bar{\nu}_\tau$ and $c\bar{s}s\bar{c}$ final states. No evidence for a signal is found. Upper limits are set on the production cross section as a function of the branching fraction $B(H^+ \to \tau^+\nu_\tau)$ and of the mass $m_{H^\pm}$, assuming that the sum of the branching ratios is equal to one. In the framework of a two-Higgs-doublet model, charged Higgs bosons with masses below 65.4 GeV/c^2 are excluded at 95% confidence level independently of the decay mode.

(Submitted to Physics Letters B)

*) See next pages for the list of authors

The ALEPH Collaboration

R. Barate, D. Decamp, P. Ghez, C. Goy, S. Jezequel, J.-P. Lees, F. Martin, E. Merle, M.-N. Minard, B. Pietrzyk

Laboratoire de Physique des Particules (LAPP), IN^{2}P^3-CNRS, F-74019 Annecy-le-Vieux Cedex, France

S. Bravo, M.P. Casado, M. Chmeissani, J.M. Crespo, E. Fernandez, M. Fernandez-Bosman, Ll. Garrido,[15] E. Graugés, J. Lopez, M. Martinez, G. Merino, R. Miquel, Ll.M. Mir, A. Pacheco, D. Paneque, H. Ruiz

Institut de Física d'Altes Energies, Universitat Autònoma de Barcelona, E-08193 Bellaterra (Barcelona), Spain[7]

A. Colaleo, D. Creanza, N. De Filippis, M. de Palma, G. Iaselli, G. Maggi, M. Maggi, S. Nuzzo, A. Ranieri, G. Raso, F. Ruggieri, G. Selvaggi, L. Silvestris, P. Tempesta, A. Tricomi,[3] G. Zito

Dipartimento di Fisica, INFN Sezione di Bari, I-70126 Bari, Italy

X. Huang, J. Lin, Q. Ouyang, T. Wang, Y. Xie, R. Xu, S. Xue, J. Zhang, L. Zhang, W. Zhao

Institute of High Energy Physics, Academia Sinica, Beijing, The People's Republic of China[8]

D. Abbaneo, G. Boix,[6] O. Buchmüller, M. Cattaneo, F. Cerutti, G. Dissertori, H. Drevermann, R.W. Forty, M. Frank, F. Gianotti, T.C. Greening, A.W. Halley, J.B. Hansen, J. Harvey, P. Janot, B. Jost, M. Kado, V. Lemaitre, P. Maley, P. Mato, A. Minten, A. Moutoussi, F. Ranjard, L. Rolandi, D. Schlatter, M. Schmitt,[20] O. Schneider,[2] P. Spagnolo, W. Tejessy, F. Teubert, E. Tournefier, A. Valassi, J.J. Ward, A.E. Wright

European Laboratory for Particle Physics (CERN), CH-1211 Geneva 23, Switzerland

Z. Ajaltouni, F. Badaud, G. Chazelle, O. Deschamps, S. Dessagne, A. Falvard, P. Gay, C. Guicheney, P. Henrard, J. Jousset, B. Michel, S. Monteil, J-C. Montret, D. Pallin, J.M. Pascolo, P. Perret, F. Podlyski

Laboratoire de Physique Corpusculaire, Université Blaise Pascal, IN^{2}P^3-CNRS, Clermont-Ferrand, F-63177 Aubière, France

J.D. Hansen, J.R. Hansen, P.H. Hansen,[1] B.S. Nilsson, A. Wäänänen

Niels Bohr Institute, 2100 Copenhagen, DK-Denmark[9]

G. Daskalakis, A. Kyriakis, C. Markou, E. Simopoulou, A. Vayaki

Nuclear Research Center Demokritos (NRCD), GR-15310 Attiki, Greece

A. Blondel,[12] J.-C. Brient, F. Machefert, A. Rougé, M. Swynghedauw, R. Tanaka H. Videau

Laboratoire de Physique Nucléaire et des Hautes Energies, Ecole Polytechnique, IN^{2}P^3-CNRS, F-91128 Palaiseau Cedex, France

E. Focardi, G. Parrini, K. Zachariadou

Dipartimento di Fisica, Università di Firenze, INFN Sezione di Firenze, I-50125 Firenze, Italy

A. Antonelli, M. Antonelli, G. Bencivenni, G. Bologna,[4] F. Bossi, P. Campana, G. Capon, V. Chiarella, P. Laurelli, G. Mannocchi,[5] F. Murtas, G.P. Murtas, L. Passalacqua, M. Pepe-Altarelli

Laboratori Nazionali dell'INFN (LNF-INFN), I-00044 Frascati, Italy

M. Chalmers, J. Kennedy, J.G. Lynch, P. Negus, V. O'Shea, B. Raeven, D. Smith, P. Teixeira-Dias, A.S. Thompson

Department of Physics and Astronomy, University of Glasgow, Glasgow G12 8QQ,United Kingdom[10]

R. Cavanaugh, S. Dhamotharan, C. Geweniger,[1] P. Hanke, V. Hepp, E.E. Kluge, G. Leibenguth, A. Putzer,

K. Tittel, S. Werner,[19] M. Wunsch[19]

Kirchhoff-Institut für Physik, Universität Heidelberg, D-69120 Heidelberg, Germany[16]

R. Beuselinck, D.M. Binnie, W. Cameron, G. Davies, P.J. Dornan, M. Girone, N. Marinelli, J. Nowell, H. Przysiezniak,[1] J.K. Sedgbeer, J.C. Thompson,[14] E. Thomson,[23] R. White

Department of Physics, Imperial College, London SW7 2BZ, United Kingdom[10]

V.M. Ghete, P. Girtler, E. Kneringer, D. Kuhn, G. Rudolph

Institut für Experimentalphysik, Universität Innsbruck, A-6020 Innsbruck, Austria[18]

C.K. Bowdery, P.G. Buck, D.P. Clarke, G. Ellis, A.J. Finch, F. Foster, G. Hughes, R.W.L. Jones, N.A. Robertson, M. Smizanska

Department of Physics, University of Lancaster, Lancaster LA1 4YB, United Kingdom[10]

I. Giehl, F. Hölldorfer, K. Jakobs, K. Kleinknecht, M. Kröcker, A.-S. Müller, H.-A. Nürnberger, G. Quast,[1] B. Renk, E. Rohne, H.-G. Sander, S. Schmeling, H. Wachsmuth, C. Zeitnitz, T. Ziegler

Institut für Physik, Universität Mainz, D-55099 Mainz, Germany[16]

A. Bonissent, J. Carr, P. Coyle, C. Curtil, A. Ealet, D. Fouchez, O. Leroy, T. Kachelhoffer, P. Payre, D. Rousseau, A. Tilquin

Centre de Physique des Particules de Marseille, Univ Méditerranée, IN^{2}P^3-CNRS, F-13288 Marseille, France

M. Aleppo, S. Gilardoni, F. Ragusa

Dipartimento di Fisica, Università di Milano e INFN Sezione di Milano, I-20133 Milano, Italy.

H. Dietl, G. Ganis, A. Heister, K. Hüttmann, G. Lütjens, C. Mannert, W. Männer, H.-G. Moser, S. Schael, R. Settles,[1] H. Stenzel, W. Wiedenmann, G. Wolf

Max-Planck-Institut für Physik, Werner-Heisenberg-Institut, D-80805 München, Germany[16]

P. Azzurri, J. Boucrot,[1] O. Callot, M. Davier, L. Duflot, J.-F. Grivaz, Ph. Heusse, A. Jacholkowska,[1] L. Serin, J.-J. Veillet, I. Videau,[1] J.-B. de Vivie de Régie, D. Zerwas

Laboratoire de l'Accélérateur Linéaire, Université de Paris-Sud, IN^{2}P^3-CNRS, F-91898 Orsay Cedex, France

G. Bagliesi, T. Boccali, G. Calderini, V. Ciulli, L. Foà, A. Giammanco, A. Giassi, F. Ligabue, A. Messineo, F. Palla,[1] G. Rizzo, G. Sanguinetti, A. Sciabà, G. Sguazzoni, R. Tenchini,[1] A. Venturi, P.G. Verdini

Dipartimento di Fisica dell'Università, INFN Sezione di Pisa, e Scuola Normale Superiore, I-56010 Pisa, Italy

G.A. Blair, J. Coles, G. Cowan, M.G. Green, D.E. Hutchcroft, L.T. Jones, T. Medcalf, J.A. Strong, J.H. von Wimmersperg-Toeller

Department of Physics, Royal Holloway & Bedford New College, University of London, Surrey TW20 OEX, United Kingdom[10]

R.W. Clifft, T.R. Edgecock, P.R. Norton, I.R. Tomalin

Particle Physics Dept., Rutherford Appleton Laboratory, Chilton, Didcot, Oxon OX11 OQX, United Kingdom[10]

B. Bloch-Devaux, D. Boumediene, P. Colas, B. Fabbro, G. Faïf, E. Lançon, M.-C. Lemaire, E. Locci, P. Perez, J. Rander, J.-F. Renardy, A. Rosowsky, P. Seager,[13] A. Trabelsi,[21] B. Tuchming, B. Vallage

CEA, DAPNIA/Service de Physique des Particules, CE-Saclay, F-91191 Gif-sur-Yvette Cedex, France[17]

S.N. Black, J.H. Dann, C. Loomis, H.Y. Kim, N. Konstantinidis, A.M. Litke, M.A. McNeil, G. Taylor

Institute for Particle Physics, University of California at Santa Cruz, Santa Cruz, CA 95064, USA[22]

C.N. Booth, S. Cartwright, F. Combley, P.N. Hodgson, M. Lehto, L.F. Thompson

Department of Physics, University of Sheffield, Sheffield S3 7RH, United Kingdom[10]

K. Affholderbach, A. Böhrer, S. Brandt, C. Grupen,[1] J. Hess, A. Misiejuk, G. Prange, U. Sieler

Fachbereich Physik, Universität Siegen, D-57068 Siegen, Germany[16]

C. Borean, G. Giannini, B. Gobbo

Dipartimento di Fisica, Università di Trieste e INFN Sezione di Trieste, I-34127 Trieste, Italy

H. He, J. Putz, J. Rothberg, S. Wasserbaech

Experimental Elementary Particle Physics, University of Washington, Seattle, WA 98195 U.S.A.

S.R. Armstrong, K. Cranmer, P. Elmer, D.P.S. Ferguson, Y. Gao, S. González, O.J. Hayes, H. Hu, S. Jin, J. Kile, P.A. McNamara III, J. Nielsen, W. Orejudos, Y.B. Pan, Y. Saadi, I.J. Scott, J. Walsh, J. Wu, Sau Lan Wu, X. Wu, G. Zobernig

Department of Physics, University of Wisconsin, Madison, WI 53706, USA[11]

[1]Also at CERN, 1211 Geneva 23, Switzerland.
[2]Now at Université de Lausanne, 1015 Lausanne, Switzerland.
[3]Also at Dipartimento di Fisica di Catania and INFN Sezione di Catania, 95129 Catania, Italy.
[4]Also Istituto di Fisica Generale, Università di Torino, 10125 Torino, Italy.
[5]Also Istituto di Cosmo-Geofisica del C.N.R., Torino, Italy.
[6]Supported by the Commission of the European Communities, contract ERBFMBICT982894.
[7]Supported by CICYT, Spain.
[8]Supported by the National Science Foundation of China.
[9]Supported by the Danish Natural Science Research Council.
[10]Supported by the UK Particle Physics and Astronomy Research Council.
[11]Supported by the US Department of Energy, grant DE-FG0295-ER40896.
[12]Now at Departement de Physique Corpusculaire, Université de Genève, 1211 Genève 4, Switzerland.
[13]Supported by the Commission of the European Communities, contract ERBFMBICT982874.
[14]Also at Rutherford Appleton Laboratory, Chilton, Didcot, UK.
[15]Permanent address: Universitat de Barcelona, 08208 Barcelona, Spain.
[16]Supported by the Bundesministerium für Bildung, Wissenschaft, Forschung und Technologie, Germany.
[17]Supported by the Direction des Sciences de la Matière, C.E.A.
[18]Supported by the Austrian Ministry for Science and Transport.
[19]Now at SAP AG, 69185 Walldorf, Germany
[20]Now at Harvard University, Cambridge, MA 02138, U.S.A.
[21]Now at Département de Physique, Faculté des Sciences de Tunis, 1060 Le Belvédère, Tunisia.
[22]Supported by the US Department of Energy, grant DE-FG03-92ER40689.
[23]Now at Department of Physics, Ohio State University, Columbus, OH 43210-1106, U.S.A.

1 Introduction

In the Standard Model, particle masses are generated via the Higgs mechanism implemented using one doublet of complex scalar fields. In this process one physical state remains in the spectrum, known as the Standard Model Higgs boson. The most important phenomenological consequence of an extended Higgs sector is the appearance of additional spin-0 states, both neutral and charged. For example, with the addition of one more doublet, five physical states remain after the spontaneous breaking of the $\mathrm{SU(2)_L \times U(1)_Y}$ symmetry: three neutral and a pair of charged Higgs bosons. Among the possible extensions of the Higgs sector, those obtained by adding more doublets are preferred because they naturally lead at tree level to $\mathrm{M_W \simeq M_Z \cos\theta_W}$, a relation very well verified by experiment.

The ALEPH data collected at centre-of-mass energies up to 184 GeV have been used in Refs. [1, 2] to search for pair production of charged Higgs bosons predicted in models with two Higgs doublets. The negative result of the search was translated into a lower limit on the $\mathrm{H^\pm}$ mass $m_{\mathrm{H^\pm}}$ of 59 $\mathrm{GeV/c^2}$ at 95% confidence level. In this paper an update of the search based on the data collected at $\sqrt{s}$ = 188.6 GeV (hereafter referred to as the 189 GeV data) is presented. The theoretical framework and underlying assumptions are the same as detailed in Refs. [1, 2]. The $\mathrm{H^+}$ is assumed to decay predominantly into $\mathrm{c\bar{s}}$ or $\tau^+\nu_\tau$ final states (and respective charge conjugates for the $\mathrm{H^-}$). Other decay modes are not considered and $\mathrm{B(H^+ \to \tau^+\nu_\tau) + B(H^+ \to c\bar{s}) = 1}$ is assumed, but the analysis is equally sensitive to other hadronic decay modes. As a consequence, $\mathrm{H^+H^-}$ pair production leads to three final states ($\mathrm{c\bar{s}s\bar{c}}$, $\mathrm{c\bar{s}\tau^-\bar{\nu}_\tau/\bar{c}s\tau^+\nu_\tau}$ and $\tau^+\nu_\tau\tau^-\bar{\nu}_\tau$) for which separate searches are performed.

This letter is organized as follows. After a brief description of the ALEPH detector in Section 2, the event selections are described in Section 3. The results and the conclusions are given in Sections 4 and 5.

2 The ALEPH detector

Only a brief description of the ALEPH subdetectors relevant for this analysis are given here. A more comprehensive description of the detector components is given in Ref. [3] and of the reconstruction algorithms in Ref. [4].

The trajectories of charged particles are measured with a silicon vertex detector, a cylindrical drift chamber, and a large time projection chamber (TPC). These are immersed in a 1.5 T axial field provided by a superconducting solenoidal coil. This system yields a resolution of $\delta p_T/p_T = 6 \times 10^{-4} p_T \oplus 0.005$ (p_T in GeV/c). Hereafter, charged particle tracks reconstructed with at least four hits in the TPC, and originating from within a cylinder of length 20 cm and radius 2 cm coaxial with the beam and centred at the nominal collision point, are referred to as *good tracks*.

The electromagnetic calorimeter, placed between the tracking system and the coil, is a highly segmented sampling calorimeter which is used to identify electrons and photons

and to measure their energies. It has a total thickness of 22 radiation lengths at normal incidence and provides a relative energy resolution of $0.18/\sqrt{E} + 0.009$ (E in GeV). The luminosity monitors extend the calorimetric coverage down to 34 mrad from the beam axis.

Muons are identified by their penetration in the hadron calorimeter, a 1.2 m thick iron yoke instrumented with 23 layers of streamer tubes, together with two surrounding layers of muon chambers. The hadron calorimeter also provides a measurement of the energy of charged and neutral hadrons with a relative resolution of $85\%/\sqrt{E}$ (E in GeV).

The calorimetry and tracking information are combined in an energy flow algorithm, classifying a set of energy flow "particles" as photons, neutral hadrons and charged particles. From these objects, jets are reconstructed with an energy resolution of $(0.60\sqrt{E} + 0.60) \times (1 + \cos^2\theta)$ where E in GeV and θ are the jet energy and polar angle, respectively.

3 Analysis

To ensure good potential for discovery, independent of the branching fraction $\mathrm{B}(\mathrm{H}^+ \to \tau^+\nu_\tau)$, three selections are defined for the topologies $\tau^+\nu_\tau\tau^-\bar{\nu}_\tau$, $\mathrm{c\bar{s}}\tau^-\bar{\nu}_\tau/\mathrm{\bar{c}s}\tau^+\nu_\tau$ (hereafter referred to as $\mathrm{c\bar{s}}\tau^-\bar{\nu}_\tau$) and $\mathrm{c\bar{s}s\bar{c}}$. The most relevant selection criteria are chosen to achieve the best expected confidence level for exclusion of a mass hypothesis of 70 GeV/c^2. Each selection is optimised individually with the most optimistic $\mathrm{B}(\mathrm{H}^+ \to \tau^+\nu_\tau)$ in each case, *i.e.*, 0%, 100% and 50% for the $\mathrm{c\bar{s}s\bar{c}}$, $\tau^+\nu_\tau\tau^-\bar{\nu}_\tau$ and $\mathrm{c\bar{s}}\tau^-\bar{\nu}_\tau$ channels, respectively.

3.1 Monte Carlo samples

Fully simulated Monte Carlo event samples reconstructed with the same program as the data have been used for background estimates, design of selections and cut optimization. Samples of all background sources corresponding to at least 20 times the collected luminosity were generated. The most important background sources are $\mathrm{e^+e^-} \to \tau^+\tau^-$, $\mathrm{q\bar{q}}$, four-fermion processes and two-photon collisions, simulated with the KORALZ [5], PYTHIA [6], KORALW [7] and PHOT02 [8] generators.

The signal Monte Carlo events were generated using the HZHA [9] generator. Samples of at least 2000 signal events were simulated for each of the various final states for charged Higgs boson masses between 50 and 75 GeV/c^2.

3.2 The $\tau^+\nu_\tau\tau^-\bar{\nu}_\tau$ final state

The final state produced by leptonic decays of both charged Higgs bosons consists of two acoplanar τ's and missing energy carried away by the neutrinos. As this topology is identical to that expected from stau pair production with massless neutralinos, the "Large ΔM" selection described in Ref. [10] is used here to search for charged Higgs bosons in this channel. Efficiencies to select events from $\mathrm{H^+H^-} \to \tau^+\nu_\tau\tau^-\bar{\nu}_\tau$ are of the

Table 1: Selection efficiencies ϵ (in %) as a function of the charged Higgs boson mass $m_{\mathrm{H}^\pm}$.

$m_{\mathrm{H}^\pm}$ (GeV/c^2)	50	55	60	65	70	75
$\epsilon\,(\tau^+\nu_\tau\tau^-\bar{\nu}_\tau)$	34	35	38	35	40	41
$\epsilon\,(\mathrm{c\bar{s}}\tau^-\bar{\nu}_\tau)$	35	37	37	35	29	20
$\epsilon\,(\mathrm{c\bar{s}s\bar{c}})$	48	48	49	49	48	45

order of 35%, as shown in Table 1 for a representative set of charged Higgs boson masses. The total expected background amounts to 15.5 events, mainly consisting of irreducible background from $\mathrm{W^+W^-} \to \tau^+\nu_\tau\tau^-\bar{\nu}_\tau$. In the data, 20 events are selected, in agreement with the expectation. The systematic uncertainty on the number of expected signal events is estimated to be 3.0%, dominated by the effect of limited Monte Carlo statistics (2.7%) and uncertainties on the cross-section for charged Higgs production (1.0%). The systematic error on the background is estimated to be 8%. This is dominated by the effect of limited Monte Carlo statistics (4%), uncertainties on the cross section for W pair production (2%), and uncertainities on the cross section for two-photon processes (7%). The systematic error on the luminosity is estimated to be 0.5%.

3.3 The $\mathrm{c\bar{s}}\tau^-\bar{\nu}_\tau$ final state

The mixed final state $\mathrm{c\bar{s}}\tau^-\bar{\nu}_\tau$ is characterised by two jets originating from the hadronic decay of one of the charged Higgs bosons and a thin jet plus missing energy due to the neutrinos from the subsequent decay of the charged Higgs and of the τ.

As a first step in the analysis the thrust of the event is required to be less than 0.96 and the total number of good charged tracks greater than 7. To reduce background from two-photon processes and the contribution of beam related background which is not simulated, the energy deposited in a 12° cone around the beam axis is required to be less than 2.5% of the centre-of-mass energy. Background from $\mathrm{e^+e^-} \to \mathrm{q\bar{q}}(\gamma)$ events is reduced by demanding that the polar angle θ_{miss} of the missing momentum vector point away from the beam axis such that $|\cos\theta_{\mathrm{miss}}| < 0.9$. To reduce the background from $\mathrm{W^+W^-} \to \mathrm{q\bar{q}}'\ell\overline{\nu}_\ell$ where ℓ corresponds to an electron or muon, it is required that the events contain no identified lepton with a momentum greater than 10% of the centre-of-mass energy.

At this point the events are clustered into three jets using the JADE algorithm [11]. The y_{cut} value where the transition from two to three jets occurs is required to be greater than 0.001. The jet with the lowest charged track multiplicity is taken as the τ jet candidate. If at least two jets have the same multiplicity the τ jet candidate is taken to be the lowest momentum jet. The following quality cuts are then applied on the τ jet. It is required that the charged multiplicity of the τ jet be between one and three. The angle between the τ jet and the closest quark jet candidate is required to be between 30° and 125°. The energy of the τ jet boosted into the charged Higgs boson rest frame, defined as the frame recoiling against the hadronic system, is required to be less than 40 GeV.

To further suppress backgrounds the following four variables are used:

- The angle $\theta_{q\bar{q}'}$ between the two hadronic jets.
- The total transverse momentum p_t^{tot} divided by the total visible energy E_{vis}.
- The cosine of the production angle of the events, reconstructed from the sum of the momenta of the two quark jets, multiplied by the charge of the τ obtained from the tracks of the τ jet, to form the variable $q_\tau \times \cos\theta_{prod}$. In the case of two tracks in the τ jet the charge of the highest momentum track is used.
- The χ^2 per number of degrees of freedom from a kinematic fit to the events using the constraints of energy and momentum conservation and the equality of the two masses produced in each side of the event.

The four variables are linearly combined in a discriminating variable D, displayed in Fig. 1a. The cut optimisation leads to $D > 0.26$. In the data collected at $\sqrt{s} = 189$ GeV, 20 events are selected, in agreement with the background expectation of 22.6. The efficiencies of selection for a range of masses are given in Table 1. The mass of the hadronic system, and hence the mass of the charged Higgs candidates, is rescaled such that the energy of the two jets is equal to the beam energy in order to improve the resolution. The reconstructed masses of the candidate events are displayed in Fig. 1b. The cutoff near 80 GeV/c^2 is due to the influence of the $\theta_{q\bar{q}'}$ variable.

The systematic uncertainty on the number of expected signal events is estimated to be 4.1%. The main contributions are from Monte Carlo statistics (3.5%), calibration uncertainties (1.5%) and uncertainty on the cross section for charged Higgs production (1.0%). The systematic error on the background level is estimated to be 12%. The main contributions are from Monte Carlo statistics (3%), uncertainty on the cross section for the W^+W^- process (2%) and from the statistics of data/Monte Carlo comparisons (10%). The systematic error on the luminosity is estimated to be 0.5%.

3.4 The $c\bar{s}s\bar{c}$ final state

The hadronic decays of two charged Higgs bosons lead to a final state of four well separated jets, which can be combined into two dijets with equal masses. With respect to Ref. [2] the preselection and jet pairing method remain unchanged.

The following five variables are used:

- The χ^2 per degree of freedom from a five-constraint kinematic fit. The constraints in the fit are from conservation of energy and momentum and the equality of the two charged Higgs masses in the event.
- The production polar angle θ_{prod}, *i.e.*, the angle between the charged Higgs boson momentum direction and the beam axis.

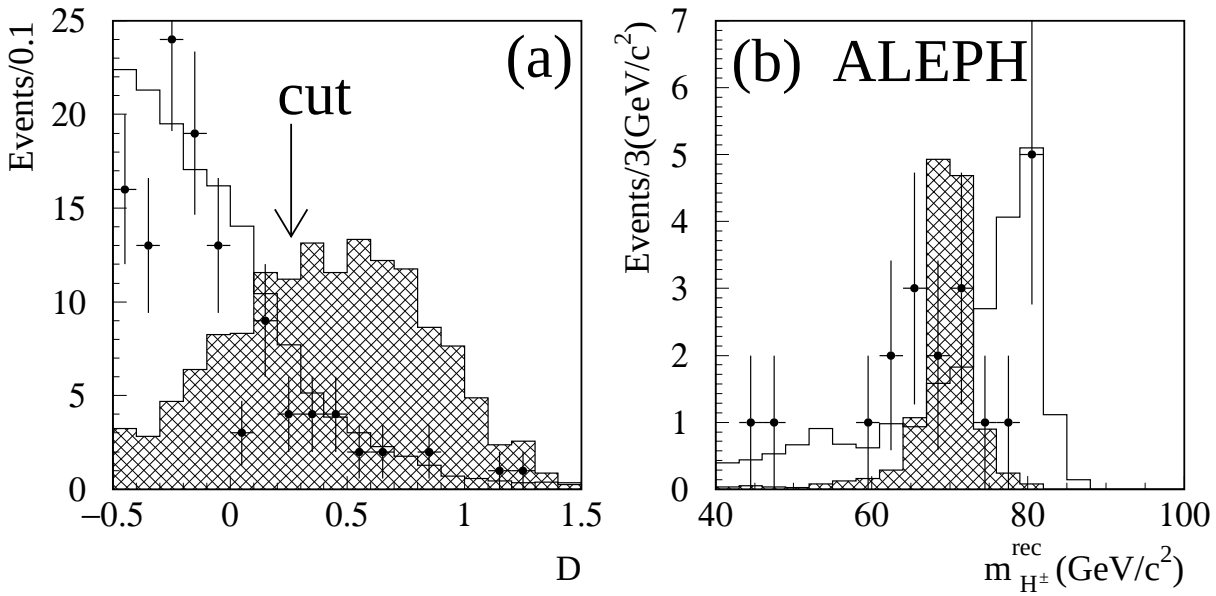

Figure 1: (a) The distribution of the discriminating variable D described in the text for the semi leptonic channel at the level of preselection. (b) The reconstructed masses of the charged Higgs candidates after the cut on the discriminating variable. In both plots the points are the data, the open histograms are the Standard Model background and the hatched areas represent the charged Higgs signal expectation with $m_{\mathrm{H}^\pm} = 70$ GeV/c^2. The signal is normalised arbitrarily in both plots.

- The difference between the largest and the smallest jet energies, $E_{max} - E_{min}$.
- The product of the minimum angle between any two jets, and the smallest jet energy, $E_{min} \times \theta_{\mathrm{q\bar{q}'}}$.
- The QCD matrix element $\mathcal{M}_{\mathrm{q\bar{q}'}}$ [12].

The variables are linearly combined into one discriminating variable D, shown in Fig. 2a. Events are accepted if $D > 4.4$. Including in D the charm tag used in Ref. [2] does not increase the discriminating power.

The analysis selects 263 events from the data for masses between 50 and 80 GeV/c^2, corresponding to a background of 294.2 events expected from Standard Model processes. The fitted-mass distribution of the selected candidates can be seen in Fig. 2b. Efficiencies are of the order of 50% as shown in Table 1.

The systematic error on the number of events expected is estimated to be 3.0%. The main contributions are from Monte Carlo statistics (2.4%), statistics of data/Monte Carlo comparison (1.2%), and knowledge of signal cross sections (1.0%). The systematic error on the background level is estimated to be 3%. The main contribution is from knowledge of the $\mathrm{W^+W^-}$ cross section (2%). The contribution of the luminosity is estimated to be 0.5%.

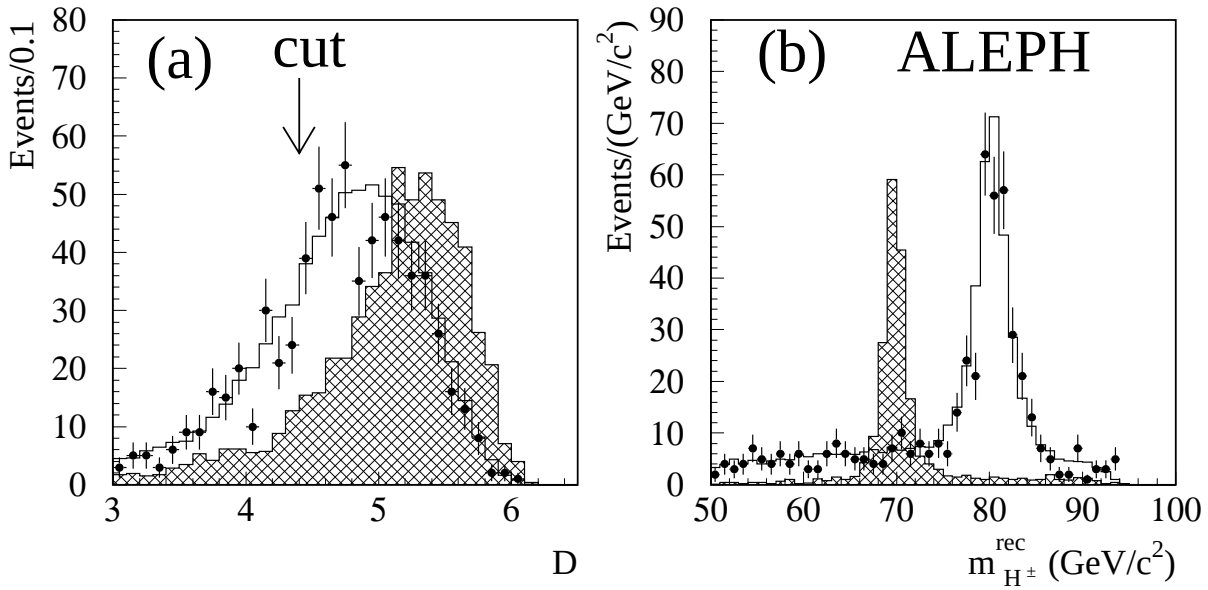

Figure 2: (a) The distribution of the discriminating variable D described in the text for the $c\bar{s}s\bar{c}$ channel at the level of preselection. (b) The distribution of the Higgs candidate masses after the cut on the discriminating variable. In both plots the points are the data, the open histograms are the Standard Model background and the hatched areas represent the Higgs signal expectation with $m_{\mathrm{H}^\pm} = 70$ GeV/c^2. The signal is normalised arbitrarily in both plots.

4 Results

The numbers of candidates observed in the data collected at a centre-of-mass energy of 189 GeV are consistent with those expected from Standard Model processes for each of the three channels. Since, in addition, the mass distributions in the $c\bar{s}s\bar{c}$ and $c\bar{s}\tau^-\bar{\nu}_\tau$ channels do not show any significant accumulation outside the $\mathrm{W}^+\mathrm{W}^-$ region (Figs. 1 and 2), the results of the three selections described in this letter are combined with those obtained using $\sqrt{s} = 172$–183 GeV data to set a 95% confidence level upper limit on the cross section for pair production of charged Higgs bosons.

In setting the limits several new features with respect to Refs. [1, 2] are to be noted. Full background subtraction is performed according to Ref. [13]. The likelihood ratio test statistic is used. The confidence levels are calculated using the semi-analytical approach described in Ref. [14]. Systematic errors are conservatively taken into account by reducing the efficiencies and subtracted backgrounds by one standard deviation. The reconstructed mass of the charged Higgs boson is used as discriminating variable for the $c\bar{s}s\bar{c}$ and $c\bar{s}\tau^-\bar{\nu}_\tau$ channels.

The upper limit on the $\mathrm{H}^+\mathrm{H}^-$ production cross section at 188.6 GeV as a function of

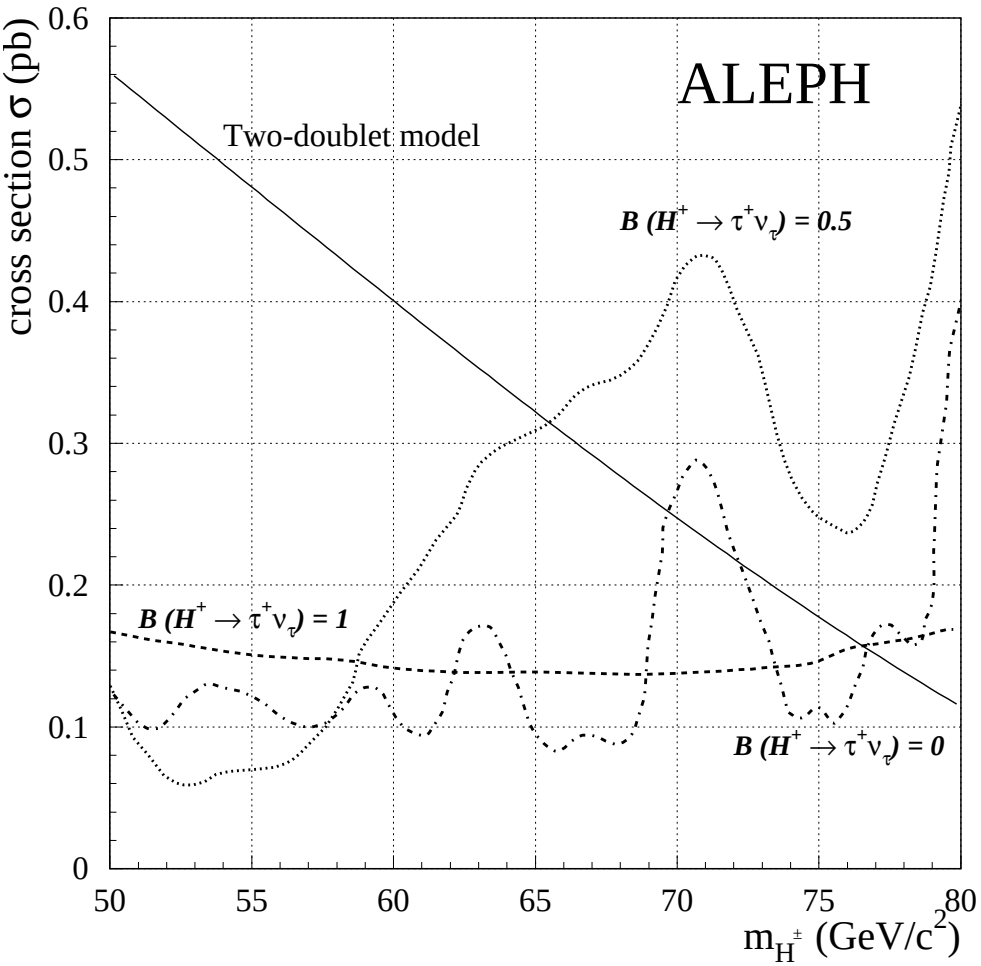

Figure 3: Upper limits at 95% confidence level on the H^+H^- production cross section at $\sqrt{s} = 188.6$ GeV for three values of $B(H^+ \to \tau^+\nu_\tau)$. The charged Higgs boson production cross section is shown as a solid curve.

$m_{H^\pm}$ is shown in Fig. 3 for three values of $B(H^+ \to \tau^+\nu_\tau)$. The results from lower centre-of-mass energies have been scaled to $\sqrt{s} = 188.6$ GeV according to the dependence of the cross section on the centre-of-mass energy.

In two-Higgs-doublet models the production cross section for H^+H^- depends, at lowest order, only on $m_{H^\pm}$. The expected cross section at 188.6 GeV, corrected for initial state radiation, is shown in Fig. 3. Upper limits on the production cross section therefore translate into excluded domains for $m_{H^\pm}$.

The result of the combination of the three analyses is displayed in Fig. 4. Charged Higgs bosons with masses less than 65.4 GeV/c^2 are excluded at 95% confidence level independently of $B(H^+ \to \tau^+\nu_\tau)$. The corresponding expected exclusion is 69.1 GeV/c^2. For the values $B(H^+ \to \tau^+\nu_\tau) = 0$, 0.5 and 1, 95% C.L. lower limits on $m_{H^\pm}$ are set at 69.9,

65.4 and 76.3 GeV/c^2, respectively.

5 Conclusions

The search for pair-produced charged Higgs bosons in the three final states $\tau^+\nu_\tau\tau^-\bar{\nu}_\tau$, $c\bar{s}\tau^-\bar{\nu}_\tau$ and $c\bar{s}s\bar{c}$ has been updated using 176.2 pb^{-1} of data collected at $\sqrt{s} = 188.6$ GeV. No evidence of charged Higgs boson production has been found and upper limits have been set on the production cross section as a function of $B(H^+ \to \tau^+\nu_\tau)$ and of $m_{H^\pm}$. Within the framework of two-Higgs-doublet models these results exclude at 95% confidence level charged Higgs bosons with masses below 65.4 GeV/c^2 independently of $B(H^+ \to \tau^+\nu_\tau)$ and assuming $B(H^+ \to \tau^+\nu_\tau) + B(H^+ \to c\bar{s}) = 1$. Similar results have been reported by L3 [15].

Acknowledgements

It is a pleasure to congratulate our colleagues from the accelerator divisions for the successful operation of LEP at high energy. We are indebted to the engineers and technicians in all our institutions for their contribution to the excellent performance of ALEPH. Those of us from non-member states wish to thank CERN for its hospitality and support.

References

[1] ALEPH Collaboration, *"Search for charged Higgs bosons in e^+e^- collisions at centre-of-mass energies from 130 to 172 GeV"*, Phys. Lett. **B 418** (1998) 419.

[2] ALEPH Collaboration, *"Search for charged Higgs bosons in e^+e^- collisions at $\sqrt{s}$ = 181-184 GeV"*, Phys. Lett. **B 450** (1999) 467.

[3] ALEPH Collaboration, *"ALEPH: a detector for electron-positron annihilations at LEP"*, Nucl. Instrum. and Methods **A 294** (1990) 121.

[4] ALEPH Collaboration, *"Performance of the ALEPH detector at LEP"*, Nucl. Instrum. and Methods. **A 360** (1995) 481.

[5] S. Jadach, B.F.L. Ward and Z. Wąs, *"The Monte Carlo program KORALZ, version 4.0, for the lepton or quark pair production at LEP/SLC energies"*, Comp. Phys. Commun. **79** (1994) 503.

[6] T. Sjöstrand, *"The PYTHIA 5.7 and JETSET 7.4 Manual"*, LU-TP 95/20, CERN-TH 7112/93, Comp. Phys. Commun. **82** (1994) 74.

[7] M. Skrzypek, S. Jadach, W. Placzek and Z. Wąs, *"Monte Carlo program KORALW-1.02 for W pair production at LEP-2/NLC energies with Yennie-Frautschi-Suura exponentiation"*, Comp. Phys. Commun. **94** (1996) 216.

[8] J.A.M. Vermasaeren, Proceedings of the IVth International Workshop on Gamma Gamma Interactions, Amiens, April 1980, Springer Verlag (Editors G.Cochard, and P.Kessler).

[9] G. Ganis and P. Janot, *"The HZHA Generator"* in *"Physics at LEP2"*, Eds. G. Altarelli, T. Sjöstrand and F. Zwirner, CERN 96-01 (1996), Vol. 2, 309.

[10] ALEPH Collaboration, *"Searches for sleptons and squarks in e^+e^- collisions at $\sqrt{s}$ = 189 GeV"*, Phys. Lett. **B 469** (1999) 303.

[11] JADE Collaboration, *"Experimental investigation of the energy dependence of the strong coupling strength"*, Phys. Lett. **B 213** 1988 (235).

[12] D. Danckaert et al., *"Four-jet production in e^+e^- annihilation"*, Phys. Lett. **114B** (1982) 203.

[13] S. Jin and P. McNamara, *"The signal estimator limit setting method"*, physics/9812030.

[14] H. Hu and J. Nielsen, *"Analytic Confidence Level Calculations using Likelihood Ratio and Fourier Transform"*, physics/9906010, submitted to Nucl. Instrum. and Methods **A**.

[15] L3 Collaboration, *"Search for Charged Higgs Bosons in e^+e^- Collisions at $\sqrt{s}$ = 189 GeV"*, Phys. Lett. **B466** (1999) 71.

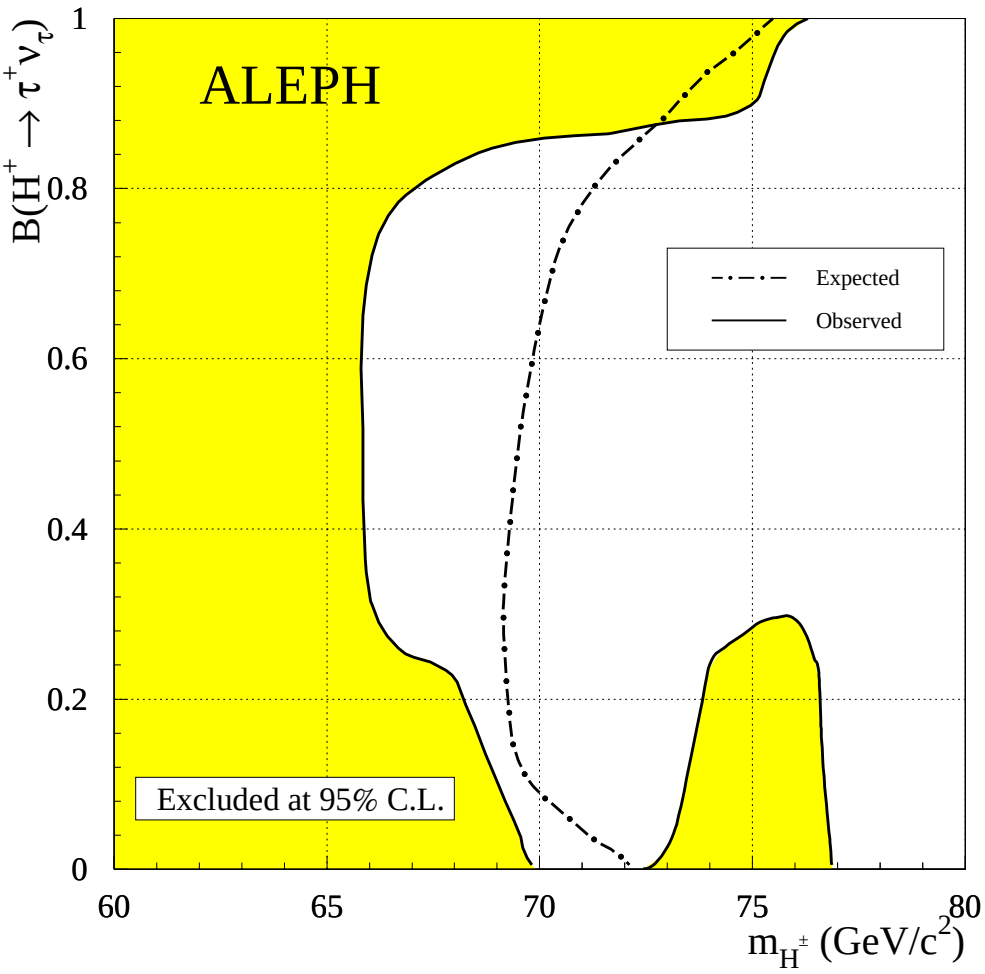

Figure 4: Limit at 95% C.L. on the mass of charged Higgs bosons as a function of $B(H^+ \to \tau^+ \nu_\tau)$. Shown are the expected (dash-dotted) and observed (solid) exclusion curves for the combination of the three analyses, and the full 172–189 GeV data set. The shaded area is excluded at 95% C.L..